Structural Engineering and Mechanics, *Vol. 60, No. 1 (2016) 31-50*
DOI: http://dx.doi.org/10.12989/sem.2016.60.1.031

A new method for progressive collapse analysis of RC frames

Reza Abbasnia[a], Foad Mohajeri Nav[*], Nima Usefi[b] and Omid Rashidian[c]

Civil Engineering Department, Iran University of Science and Technology, Narmak, Tehran, Iran

(Received January 4, 2015, Revised July 11, 2016, Accepted July 12, 2016)

Abstract. During the recent years, resistance mechanisms of reinforced concrete (RC) buildings against progressive collapse are investigated extensively. Although a general agreement is observed about their qualitative behavior in technical literature, there is not such a comprehensive point of view regarding the quantitative methods for predicting collapse resistance of RC members. Therefore, in the present study a simplified theoretical method is developed in order to predict general behavior of RC frames under the column removal scenario. In the introduced method, the robustness of the frame is extracted based on the capacity of the beams. The proposed method expresses ultimate arching and catenary capacities of the beams and also obtains the corresponding vertical displacements. Based on the calculated capacities, the introduced method also provides a quantitative assessment of structural robustness and determines whether or not the collapse occurs. The capability of the method is evaluated using experimental results in the literature. The evaluation study indicates that the proposed theoretical procedure can establish a reliable foundation for progressive collapse assessment of RC frame structures.

Keywords: progressive collapse analysis; RC beam; RC frame; compressive arch action; catenary action; structural robustness

1. Introduction

Progressive collapse is occurred due to an initial local failure in a structure and its spread to other parts which finally leads to disproportionate collapse of the entire structure (ASCE/SEI 7-10, 2010). The collapses of the Ronan Point Tower in London in 1968, the Alfred P. Murrah Federal Building in Oklahoma City in 1995 and the World Trade Center in New York in 2001 are the most known examples during the past decades.

Recently, extensive researches were performed in order to understand the behavior of reinforced concrete (RC) structures against progressive collapse. Among different studies, Sasani *et al.* (2007, 2008, 2009, 2010, 2011) carried out a great effort to investigate the collapse behavior of full scale reinforced concrete structures. A 10 story RC building which belonged to University of Arkansas Medical Center Dormitory (Sasani *et al.* 2007), a 6 story RC building of Hotel San

∗Corresponding author, Ph.D., E-mail: foadmohajeri@iust.ac.ir
[a]Professor, E-mail: abbasnia@iust.ac.ir
[b]M.Sc. Student, E-mail: N_yusefi@civileng.iust.ac.ir
[c]Ph.D. Candidate, E-mail: omidrashidian@iust.ac.ir

http://www.techno-press.org/?journal=sem&subpage=8 ISSN: 1225-4568 (Print), 1598-6217 (Online)

Diego (Sasani 2008, Sasani and Sagiroglu 2008a, b), a 11 story RC building (Sasani *et al.* 2011) and also a 20 story RC building (Sasani and Sagiroglu 2010), were the most important studies. In all the cases, compressive arch action (CAA) of beams, Vierendeel (frame) action of beams and columns and also catenary action of longitudinal reinforcements were the main resistance mechanisms against progressive collapse. Yi *et al.* (2008) performed laboratory testing of a RC four bays and three stories planar frame where the static responses were examined under the progressive collapse. In their study, one of the middle columns in the ground level was removed and a constant vertical load was applied to the top of the middle column to simulate progressive failure of the frame. Almusallam *et al.* (2010) evaluated an existing RC building under the progressive collapse analysis due to the blast loading. In their study, a commercial RC building was analyzed under the different blast scenarios using finite element method. Karimiyan *et al.* (2014) evaluated collapse resistance of regular and irregular 6-story RC ordinary moment resisting frame buildings under the earthquake loads. Su *et al.* (2009) evaluated the load-carrying capacity of RC sub-assemblages against progressive collapse. They tested twelve reduced-scale specimens where the beams were restrained longitudinally against axial deformation. The results showed that the compressive arch action due to the longitudinal restraint can significantly enhance the load-carrying capacity of the assembly. Kim *et al.* (2014) evaluated the role of MR dampers in preventing progressive collapse of moment frames. In an experimental research, Lew *et al.* (2014) studied behavior of two full scale RC sub-assemblages subjected to static loading. In these tests similar to the previous researches, resistance of sub-assemblages was based on arching and catenary actions. Bao *et al.* (2014) performed a computational investigation of the same assemblies and developed two types of models, a detailed model and a reduced model. The sub-assemblages which were tested by Lew *et al.* (2014) were used to validate these models. In an extensive research, Qian and Li (2012, 2013a, b) investigated the behavior of RC frames under the loss of a corner column. Bao *et al.* (2008), Bao and Kunnath (2010) developed macro-models in order to study the progressive collapse behavior of RC frames. Sasani *et al* (2011b) introduced detailed models for modeling the bar fractures in RC frames under the progressive collapse. Yu and Tan (2011) performed an experimental testing of two half scale RC sub-assemblages under a middle column removal scenario. In a further investigation, Yu and Tan (2013) studied the collapse resistance of six new RC sub-assemblages under the same conditions. Yu *et al*. (2014) also performed laboratory testing of three half scale RC sub-assemblages subjected to blast loading. In these studies, catenary and compressive arch actions observed as the resistance mechanisms. Li and Hao (2013) developed a new numerical approach based on finite element (FE) model to simulate progressive collapse resistance of structures under the blast loading. Long *et al*. (2013) proposed an integrated super-element concept which can be used in finite element programs in order to perform progressive collapse analysis of large scale structures. Qian *et al.* (2014) investigated the effects of transverse beams and slabs. Stinger and Orton (2013) tested a part of a RC frame and investigated the performance of different resistance mechanisms. Tavakoli and Akbarpoor (2014) investigated seismic performance and shear strength of R.C frames with brick infill panel under various lateral loading patterns.

Although general behavior of RC structures is known, still there is a long running debate about the precise estimation of their resistance against progressive collapse. Jian and Zheng (2014) developed a simplified method to predict the capacity curve of RC sub-assemblages. In their method, the compressive arch capacity was calculated based on classical beam mechanism and hence, role of arching action in increasing the ultimate capacity was neglected. Also in different researches, such as Yi *et al.* (2008), Su *et al.* (2009), Yu and Tan (2011, 2013), many formulations are developed in order to predict the catenary capacity of beams, but even in these studies there is not a general agreement. In some studies (Yu and Tan 2011, 2013), catenary capacity is estimated based on the strength of top bars while in others (Yi *et al.* 2008, Su *et al.* 2009) bottom bars are playing the major role. Furthermore, prediction of the compressive arch action was not discussed in these studies. Lately, Yu and Tan (2014) developed an analytical model to predict the CAA capacity of RC sub-assemblages under the middle column removal. Their method is a repetitive approach which only focuses on CAA stage. In other attempts in order to quantify the structural resistance against progressive collapse, Menchel *et al.* (2011) developed an equivalent static pushover procedure which utilizes a kinetic energy criterion but it is only evaluated using steel structures. Weerheijm *et al.* (2009) also tried to quantify the response and residual bearing capacity of RC elements and structures against blast loading.

Based on a comprehensive review of progressive collapse of structures which is performed by Yagob *et al.* (2009), efficient and inexpensive design methods are needed in order to provide resistance structures against abnormal loading events. More recent studies (Jian and Zheng 2014, Yu and Tan 2014) also demonstrate the same trend among researchers. Hence, in order to predict the behavior of RC frames under the column removal scenario, the present study introduces a theoretical and non-repetitive method. In the proposed method, arching and catenary capacities of RC beams in a frame and also the corresponding displacements are calculated and the robustness of the frame under a column removal scenario is evaluated based on the obtained capacities. Compressive arch capacity and catenary capacity of RC beams are computed separately using theoretical concepts. The robustness of the RC frames is assessed based on the arching and catenary resistance of the beams. Influences of beam dimensions, spans and longitudinal reinforcements are taken into account. The proposed method is validated by experiments in the literature. Evaluations demonstrate that the proposed method is a useful tool for estimating collapse resistance of RC structures.

2. The proposed model

2.1 General concept

Generally a column removal scenario is adopted in order to simulate the progressive collapse phenomenon in a building. By removing a column in a RC frame, the connected beams firstly resist against collapse based on flexural and compressive arch actions. As the displacement of the joint above the removed column increases, flexural cracks are formed and developed at two ends of the beams. At this stage, concrete begins to crush at the top of the beams next to the removed column. Resistance of beams during the compressive arch stage is mostly due to the compressive axial forces which could enhance the ultimate flexural strength of a section. Restraining axial deformation in the beams causes these compressive axial forces. With a further increment in the vertical displacement, axial forces of the beams change gradually from compression to tension. Due to tension axial forces in the beams, the catenary stage starts. Since concrete cannot bear tension, forces are transferred through the longitudinal reinforcements. Experiments (Yu and Tan 2011, 2013) showed that when the vertical displacement is more than the beam's depth, compressive arch action is replaced by catenary action. Following this replacement, extensive tensional cracks develop along the beam and perpendicular to beam axis. Two wide cracks develop at two sides of the joint which leads to strain concentration and gradual fracture of steel bars. Once

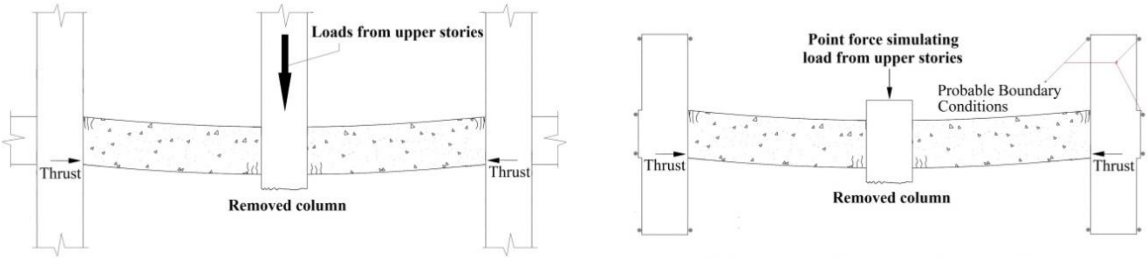

(a) a real RC frame (b) an equivalent RC sub-assemblage

Fig. 1 Progressive collapse in (a) a real RC frame; (b) an equivalent RC sub-assemblage

the displacement of the joint above the removed column reaches to 10% of the total length of two bays, maximum catenary action and also the fracture of bars in tension would take place (Yu and Tan 2013).

The present paper firstly focuses on calculating ultimate capacities and corresponding displacements of RC beams within a frame under a middle column removal scenario. Hence, the following assumptions are considered in the development of the theoretical approach:

(a) Maximum moment due to the arching mechanism occurs after the initial yielding in longitudinal bars;

(b) Flexural deformations is neglected in comparison to large displacements due to the progressive collapse;

(c) Crack patterns and failure modes at two sides of the removed column is symmetrical;

(d) Depth of compression zone at two ends of the beams connected to the removed column is similar.

(e) Dynamic conditions, including high strain rates and inertial effects are neglected in the proposed model;

(f) Effects of shear stirrups are neglected in the development of the model;

Since resistance of beams is the main purpose of the present study, the effects of floor in RC frames are neglected according to Fig. 1(a). Hence, an idealized sub-assemblage including three columns and two beams according to Fig. 1(b) is chosen as a basis for developing the theoretical method. This idealized sub-assemblage is used in many studies (Lew *et al.* 2014, Bao *et al.* 2008. 2014, Yu and Tan 2011, 2013, 2014, Jian and Zheng 2014, etc.). In addition, it should be mentioned that the proposed method is based on the removal of a middle column or an external column (neglecting the effects of transverse beams and slabs) and it cannot be used for corner column removal scenarios. Therefore, the joint above the removed column is called *the middle joint* in this paper. Moreover, the method is developed for static conditions and the effects of dynamic loading and high strain rates are also neglected.

Calculation of ultimate arching and catenary capacities and also corresponding vertical displacements of an RC sub-assemblage is described separately in the following sections and finally robustness of the total frame is discussed.

2.2 Compressive arch stage

Compressive arch action occurs due to the considerable difference between tensile and compressive strengths of concrete. When a column is removed, cracking of concrete occurs at two

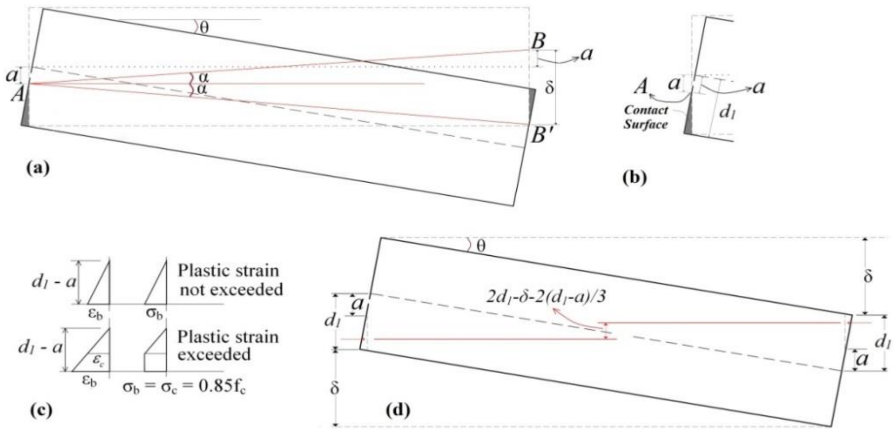

Fig. 2 Geometry of deformations and stress distributions at two ends of the beam

sides of the middle joint and leads to movement of neutral axis. Consequently, connected beams tend to elongate but other beams and columns within the frame restrain this elongation. This process leads to development of compressive arch action which provides an enhancement in the strength of beams.

Arching action firstly investigated in masonry walls (McDowell *et al.* 1956) and RC slabs (Christiansen 1963, Rankin and Long 1997, etc.). In the present study, a method which is developed by Rankin and Long (1997) is modified in order to calculate the arching capacity in RC beams. Based on the modified method, two states are defined for concrete at two ends of each beam which is connected to the removed column: maximum strain (ε_b) is (1) less than the plastic strain; or (2) greater than the plastic strain. The shaded area in Fig. 2(a) and (b) depicts concrete in compressive zone at two ends of the beam, and Fig. 2(c) demonstrates stress and strain distributions at the mentioned states. The plastic strain (ε_c) is defined based on the conventional parabolic and rectangular stress block parameters (Hognestad *et al.* 1955, Mattock *et al.* 1961) according to Eq. (1). The basic assumptions in conventional flexure theory are still valid here (Hognestad *et al.* 1955 and Mattock *et al.* 1961).

$$\varepsilon_c = (-400 + 60f_c - 0.33f_c^{\,2}) \times 10^{-6} \tag{1}$$

where f_c (MPa) is the compressive strength of the concrete. Fig. 2(d) demonstrates the calculated lever arm for the first state of strain. The corresponding lever arm for the second state can be calculated in a similar way. Consequently, a separate relationship for arching moment (M_u) at each state is obtained. The final relations are summarized in Table 1 based on three dimensionless parameters (R, u and M_r). Eqs. (2)-(3) define these parameters. It should be mentioned that these dimensionless parameters are only defined for simplifying the relations and hence, they do not represent structural concepts.

$$\begin{cases} R = \dfrac{\varepsilon_c L^2}{4d_1^2} & (a) \\ u = \dfrac{\delta}{2d_1} & (b) \end{cases} \tag{2}$$

Table 1 Analysis of arching moment (McDowell *et al.* 1956)

Strain Condition	Stress Distribution	$M_r=\dfrac{4M_u}{\sigma_c d_1^2}$
$\varepsilon_{b\,\max}<\varepsilon_c$	triangular	$\dfrac{8u}{3R}\left(1-\dfrac{u}{2}\right)^2\left(1-\dfrac{5u}{4}\right)$
$\varepsilon_{b\,\max}\geq\varepsilon_c$	trapezoidal	$4\left(1+\dfrac{R}{2}+\dfrac{3u^2}{4}-2u-\dfrac{R^2}{3u^2}\right)$

$$M_r=\frac{4M_u}{\sigma_{cc}d_1^2} \tag{3}$$

where L is the beam span; $2d_1$ is the depth of arching section; δ is the deflection at the middle joint; σ_{cc} is the maximum stress in concrete; and M_u and M_r are arching moment and arching moment ratio, respectively. In order to obtain the maximum arching moment ratio, the presented equations are differentiated with respect to u. According to Christiansen (1963), $2d_1$ is the available height which takes part in arching action and is calculated using Eq. (4)

$$2d_1=h-(\rho+\rho')\frac{f_y d}{0.85f_c} \tag{4}$$

Based on discussions by McDowell *et al.* (1956), Rankin and Long (1997), a polynomial relationship between M_r and R is derived according to Eq. (5)

$$M_r=\begin{cases}4.3-16.1\sqrt{3.3\times10^{-4}+0.1243R} & 0<R<0.26\\ \dfrac{0.3615}{R} & R>0.26\end{cases} \tag{5}$$

Proceeding the mentioned procedure, for R>0.26 plastic strain in concrete is not exceeded and for $0<R<0.26$ it is exceeded. Regarding the maximum stress in the concrete ($\sigma_{cc}=0.85f_c$), the maximum arching moment (M_{CAA}) per unit width of the beam is calculated using Eq. (6)

$$M_{CAA}=\frac{0.85f_c\,\mathrm{d}_1^2}{4}\frac{l_e}{L_r}M_r \tag{6}$$

where l_e is half span of elastically-restrained strip in Rankin's method which herein is equal to beam's net span. Based on Rankin's theory, the longer equivalent rigidly restrained slab has been used to describe the load-deformation response of a shorter finitely restrained slab. Hence, herein an equivalent rigidly restrained beam (L_r), according to Eq. (7), is used in order to estimate the behavior of the corresponding finitely restrained beam. Equivalent rigidly restrained beam is the equivalent beam which is constrained between two rigid supports.

$$L_r=l_e\sqrt[3]{\frac{E_cA}{Kl_e}+1} \tag{7}$$

where E_c is the short-term static elastic modulus of concrete, A is the cross-sectional area of the

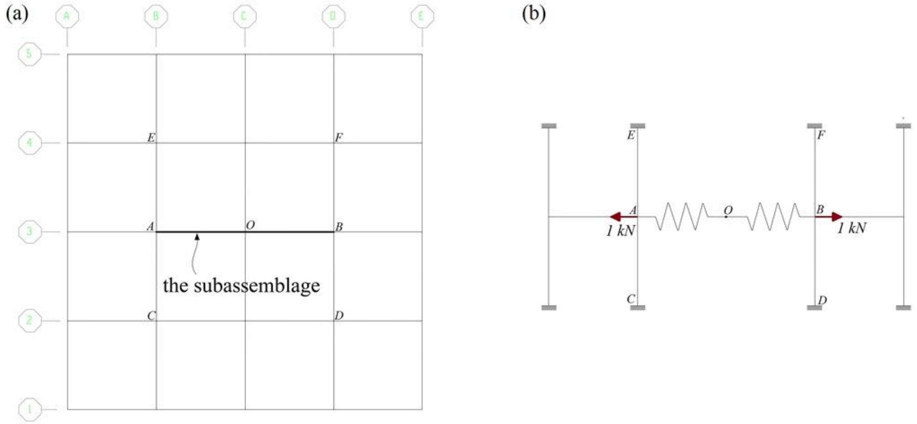

Fig. 3 Frame analysis of the sub-assemblage to determine the restraint stiffness; (a) Original plan; (b) Corresponding model for linear-elastic analysis

beam, and K is the stiffness of elastic spring restraint.

Eq. (7) requires a value for the lateral restraint stiffness, K. Hon *et al.* (2005) developed a method for estimating the lateral restraint stiffness based upon a simple frame model of a slab which is modified here for a RC sub-assemblage. They modeled the axial stiffness of the slab as a number of springs, with the stiffness of each spring dependent on the width of the slab deck. In order to adapt this method, axial stiffness of each beam in the sub-assemblage is modeled as a separate spring. The adjacent members of the sub-assemblage are modeled with fixed end rotation (The connections are assumed to be rigid). A horizontal unit load is then applied to the edge columns and the displacement obtained using a linear-elastic analysis. Hence, the horizontal translational restraint stiffness can be determined. The general concept of the method is shown in Fig. 3.

The equivalent vertical load (P_{CAA}) corresponding to the maximum arching moment is calculated based on the classic structural analysis which is presented in Eq. (8). It should be noted that the maximum arching moment equivalent to total width of the beam is used to obtain P_{CAA}.

$$P_{CAA} = \frac{4M_{CAA}}{l_n + l_{n'}} \tag{8}$$

The ultimate capacity of beams during the compressive arch stage is caused by arching and flexural actions. Since the ultimate arching strength is calculated using Eq. (8), it is only needed to compute the flexural resistance of RC beams. Hence, classical structural theories are used in order to determine the flexural resistance of the beams and the equivalent vertical load (P_f) is also calculated based on the vertical equilibrium of beams according to Eq. (9)

$$P_f = \left\{ \frac{M_{P1} + M_{P2}}{l_n} + \frac{M_{P1'} + M_{P2'}}{l_{n'}} \right\} \tag{9}$$

where M_{P1} and M_{P2} are plastic moments at two ends of the first beam; M_{P1} and M_{P2} are plastic moments at two ends of the second beam; and, l_n and $l_{n'}$ are bay lengths of the beams. Consequently, the ultimate arching capacity (P_u) is computed using Eq. (10)

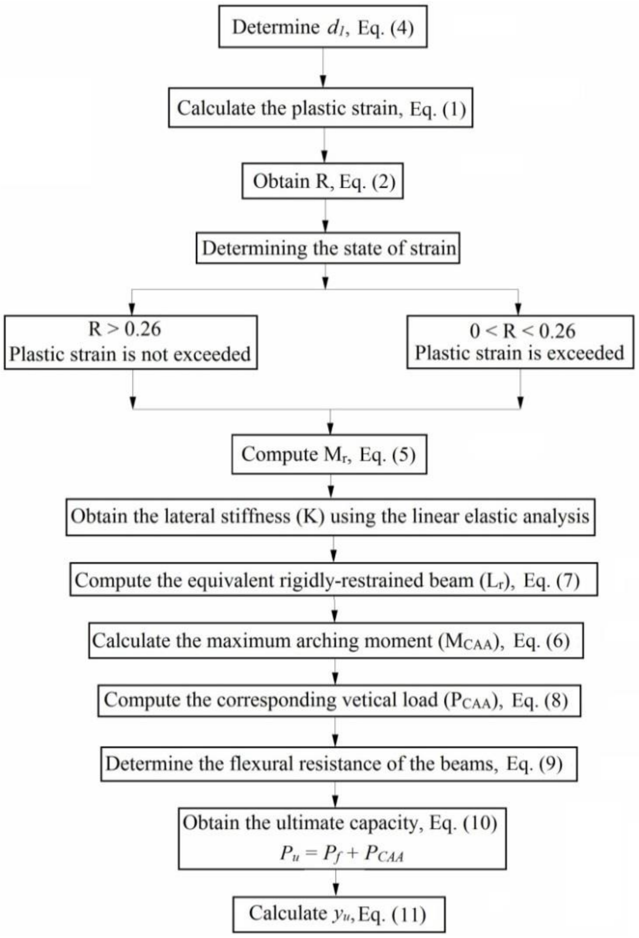

Fig. 4 The procedure for obtaining arching capacity and corresponding vertical displacement

$$P_u = P_f + P_{CAA} \tag{10}$$

Vertical displacement (y_u) corresponding to arching capacity is also calculated based on Eq. (11) which is resulted from Eq. (2)

$$y_u = 2uD \tag{11}$$

where D is half of the effective depth of the beam. This displacement is calculated for the middle joint. Fig. 4 summarizes the described procedure.

2.3 Catenary stage

Due to the negative flexural moment at the sections next to the joints along the beam, generally bottom bars are less than top bars at two sides of a joint under normal conditions. Furthermore during the catenary action two wide cracks develops at two sides of the middle joint which lead to strain concentration and bar fractures (Yi *et al.* 2008, Lew *et al.* 2014, Yu and Tan 2013). Since

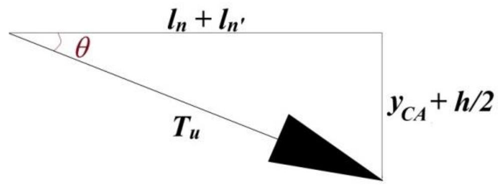

Fig. 5 An equivalent angel

bottom bars are less than top, mostly the fracture occurs at bottom bars.

According to experiments (Yu and Tan 2011, 2013), the middle joint cannot rotate freely toward the weaker side due to the rotational constraints of upper columns. Hence, during the progressive collapse in real frames, bottom bars will either rupture or pull out. Based on this fact, some studies neglect the effect of bottom bars in calculating catenary capacity of RC beams (Yu and Tan 2013). Based on experiments (Su *et al.* 2009, Lew *et al.* 2014, Yu and Tan 2013), a beam with more bottom bars would have more catenary resistance. As an example, in two beams with similar elements sizes and also similar top bars next to the middle joint, the specimen with more bottom bars would have more catenary capacity (Su *et al.* 2009). The reason is related to the direct participation of bottom bars in tension. The role of bottom bars are such important that in some researches (Yi *et al.* 2008, Su *et al.* 2009), catenary capacity is calculated based on the resistance of bottom bars. Some other researches consider both bottom and top bars (Jian and Zheng 2014). Regarding these researches, in the present study all longitudinal reinforcements are considered in developing catenary forces. In addition, the rotation of beams after the column removal is discussed in many studies (Su *et al.* 2009, Yu and Tan 2011, 2013, etc.). Hence, in the present study an equivalent angel (θ) is defined according to Eq. (12) which determines the general trend of the catenary forces with respect to the horizontal axis. Fig. 5 depicts the equivalent angel where T_u is the tensile strength of longitudinal reinforcements, y_{CA} is the vertical displacement of the middle joint corresponding to the catenary capacity and h is depth of the beam.

As discussed, both bottom and top bars are transferring tensional forces in the catenary stage. Hence, tensile resistance (T_u) of the longitudinal reinforcements is calculated based on their ultimate strength, according to Eq. (12)

$$T_u = 2\left(A_{s_{top}} f_{u_{top}} + A_{s_{bot}} f_{u_{bot}}\right) \tag{12}$$

where $A_{s_{top}}$ and $f_{u_{top}}$ are the area and ultimate strength of top bars next to the middle joint; and $A_{s_{bot}}$ and $f_{u_{bot}}$ are the area and ultimate strength of bottom bars next to the middle joint. Since two beams are existed at two side of the middle joint, the ultimate strength of bars is multiplied by two. According to Fig. 5, the vertical component of the tensile resistance is equal to the ultimate catenary capacity (P_{CA}) of the beams connected to the removed column. This vertical capacity could be extracted using Eq. (13)

$$P_{CA} = T_u \sin\theta \tag{13}$$

where $sin\theta$ is calculated according to Eq. (14)

$$\sin\theta = \frac{y_{CA} + h/2}{l_n + l_{n'}} \tag{14}$$

According to experiments (Yu and Tan 2011, 2013), when the vertical displacement of the middle joint reaches to 10% of two bay lengths, catenary capacity of the beams occurs. Therefore, corresponding vertical displacement (y_{CA}) is computed using Eq. (15)

$$y_{CA} = 0.1(l_n + l_{n'}) \tag{15}$$

2.4 Robustness of the frame

The main issue in progressive collapse analysis of RC frames is lack of a tangible way in order to convert the ultimate capacity of the beams to resistance of the total frame under a column removal scenario. Hence, the goal of this section is to provide a practical tool in order to perform a quantitative assessment of a RC frame based on the ultimate capacities of the beams. Following this purpose, two non-dimensional parameters, λ_1 and λ_2 are defined according to Eqs. (23)-(24)

$$\lambda_1 = N \Big/ \phi \sum_{i=1}^{n} P_u^{(i)} \tag{16}$$

$$\lambda_2 = N \Big/ \phi \sum_{i=1}^{n} P_{CA}^{(i)} \tag{17}$$

where N is the axial force in the removed column before the elimination; $P_u^{(i)}$ and $P_{CA}^{(i)}$ are the compressive arch capacity and the catenary capacity of RC beams at ith story; n is the number of stories above the removed column; ϕ is a reduction factor equals 0.9; and λ_1 and λ_2 are the arching and catenary ratios, respectively. Since all the beams above the removed column in a two-dimensional frame will take apart in resisting against progressive collapse, they are considered in the presented formulations. According to the experimental observations (Sasani and Sagiroglu 2008b, Sasani *et al*. 2011b) the vertical displacement above the removed column decreases in upper stories due to column elongation and, necessarily, the ultimate capacity of the beams in different stories does not occur simultaneously. In other words, whereas beams in upper stories could sustain more loads, the beams of lower stories have reached their capacity due to the larger vertical displacements. Therefore, some of the beams will not reach their ultimate capacity and the summation of flexural moments developed at the ends of these beams could be estimated at about 90 % of the expected theoretical capacity. This is obtained based on an evaluation performed on the extracted moment diagrams for RC frames available in the literature (Sasani and Sagiroglu 2008b, Sasani *et al.* 2011b). Hence, a reduction factor of 0.9 is utilized.

According to the developed formulation, $\lambda_1 \leq 1$ indicates that the frame is able to resist against progressive collapse based on the compressive arch capacity of the beams. Similarly, $\lambda_1 > 1$ and $\lambda_2 \leq 1$ denotes that the frame is able to withstand the column removal based on the catenary capacity of the beams and finally, $\lambda_1 > 1$ and $\lambda_2 > 1$ indicates that the beams connected to the removed column will fail and the frame cannot redistribute the unbalanced force resulting from the column removal. Hence the collapse extends to other parts of the building.

It should be noted that in the development of the present model, only the resistance of the beams in the plane of the frame is considered. This decision is made due to the lack of the experimental models including transvers beam. However, the presented framework could be utilized separately for calculating arching and catenary capacities of the transverse beams and these additional capacities could be added to obtain the ultimate resistance of the building. This procedure neglects the effects of the slabs.

3. Validation study

3.1 Ultimate resistances

The capability of the proposed method is validated by thirteen RC sub-assemblages in the literature. Each sub-assemblage comprises three columns and two beams and their progressive collapse behavior was studied experimentally under the middle column removal. Table 2 lists the general description of these sub-assemblages. More details can be found in the references. Quantitative comparison of the theoretical and experimental results is presented in Table 3. The translational restraint stiffnesses (K) which are calculated based on the analytical procedure are also listed in Table 3.

According to Table 3, the mean (theoretical to experimental) values for predicting compressive arch capacity (P_u) and catenary capacity (P_{CA}) are 0.947 and 0.931, respectively. The corresponding values for predicting vertical displacements are 0.934 and 0.872, respectively. Correlation coefficient (Corr.) which indicates the discrepancy between theoretical and experimental values are about 0.903 and 0.999 for predicting vertical displacements and loads corresponding to arching capacity. Also in the catenary stage, 0.966 and 0.998 are obtained as the correlation values for vertical displacements and mid-span loads, respectively. Fig. 6 also demonstrates the discrepancy between theoretical and experimental results. Regarding the results,

Table 2 Specifications of tested sub-assemblages

Reference	Model	Beam Span (m)	Material Properties			Sections at two ends of the beam		
						$b \times h$ (cm)	Reinforcement (mm)	
			f_c (MPa)	f_y (MPa)	f_u (MPa)		Top	Bottom
Yu and Tan (2013)	S1	2.750	38.2	511 (T10) & 494 (T13)	610	15×25	1T13+2T10	2T10
	S2	2.750	38.2	511	623	15×25	3T10	2T10
	S3	2.750	38.2	511 (T10) & 494 (T13)	494	15×25	3T13	2T10
	S4	2.750	38.2	494	593	15×25	3T13	2T13
	S5	2.750	38.2	494	593	15×25	3T13	3T13
	S6	2.750	38.2	494 (T13) & 513 (T16)	612	15×25	3T16	2T13
	S7	2.150	38.2	494	593	15×25	3T13	2T13
	S8	1.550	38.2	494	593	15×25	3T13	2T13
Lew *et al.* (2014)	IMF	5.385	32.0	476 (T25) & 462 (T29)	648	70×50	4T25	2T29
	SMF	5.232	36.0	476	648	86×66	7T25	6T25
Qian *et al.* (2014)	P1	1.900	19.9	437	568	10×18	2T10	2T10
	P2	1.300	20.8	437	611	8×14	2T10	2T10
Stinger and Orton	M	1.435	24.9	565	655	7.6×15	4T6.3	3T6.3

Table 3 Theoretical (Theo.) results in comparison to Experimental (Exp.) responses

Model	Result	K (N/mm)	Compressive Arch Capacity		Catenary Action	
			y_u (mm)	P_u (kN)	y_{CA} (mm)	P_{CA} (kN)
S1	Experimental	1.06E+05	78.0	41.64	573.0	68.91
	Theoretical		71.3	41.97	575.0	66.83
	Theo./Exp.		0.914	1.008	1.003	0.970
S2	Experimental	1.06E+05	73.0	38.38	612.0	67.63
	Theoretical		71.3	38.69	575.0	59.57
	Theo./Exp.		0.977	1.008	0.940	0.881
S3	Experimental	4.29E+05	74.4	54.47	729.3	124.37
	Theoretical		71.3	49.13	575.0	71.76
	Theo./Exp.		0.958	0.902	0.788	0.577
S4	Experimental	4.29E+05	81.0	63.22	614.3	103.68
	Theoretical		71.3	55.13	575.0	95.82
	Theo./Exp.		0.880	0.872	0.936	0.924
S5	Experimental	4.29E+05	74.5	70.33	665.9	105.07
	Theoretical		71.3	62.38	575.0	114.99
	Theo./Exp.		0.957	0.887	0.863	1.094
S6	Experimental	4.29E+05	114.5	70.33	675.3	143.28
	Theoretical		71.3	68.71	575.0	128.21
	Theo./Exp.		0.623	0.977	0.851	0.895
S7	Experimental	4.29E+05	74.4	82.82	628.5	105.99
	Theoretical		63.6	74.29	455.0	100.33
	Theo./Exp.		0.855	0.897	0.724	0.947
S8	Experimental	4.29E+05	45.9	121.34	504.1	91.83
	Theoretical		41.6	107.51	335.0	108.08
	Theo./Exp.		0.906	0.886	0.665	1.177
IMF	Experimental	5.06E+05	127.0	296.00	1086.5	547.00
	Theoretical		111.3	339.14	1077.0	528.90
	Theo./Exp.		0.876	1.146	0.991	0.967
SMF	Experimental	5.06E+05	112.0	903.00	1215.2	1232.01
	Theoretical		111.2	916.13	1047.0	1123.10
	Theo./Exp.		0.993	1.015	0.862	0.912
P1	Experimental	1.00E+06	46.7	32.00	370.1	47.00
	Theoretical		52.7	29.68	380.0	44.14
	Theo./Exp.		1.129	0.928	1.027	0.939
P2	Experimental	1.00E+06	33.1	36.00	299.0	59.00
	Theoretical		40.3	30.86	260.0	48.73
	Theo./Exp.		1.218	0.857	0.870	0.826
M	Experimental	1.00E+06	51.5	25.81	350.0	36.90
	Theoretical		44.1	24.08	287.0	36.75
	Theo./Exp.		0.856	0.933	0.820	0.996
	Mean Theo./Exp.		0.934	0.947	0.872	0.931
	Corr. (Theo. and Exp.)		0.903	0.999	0.966	0.998

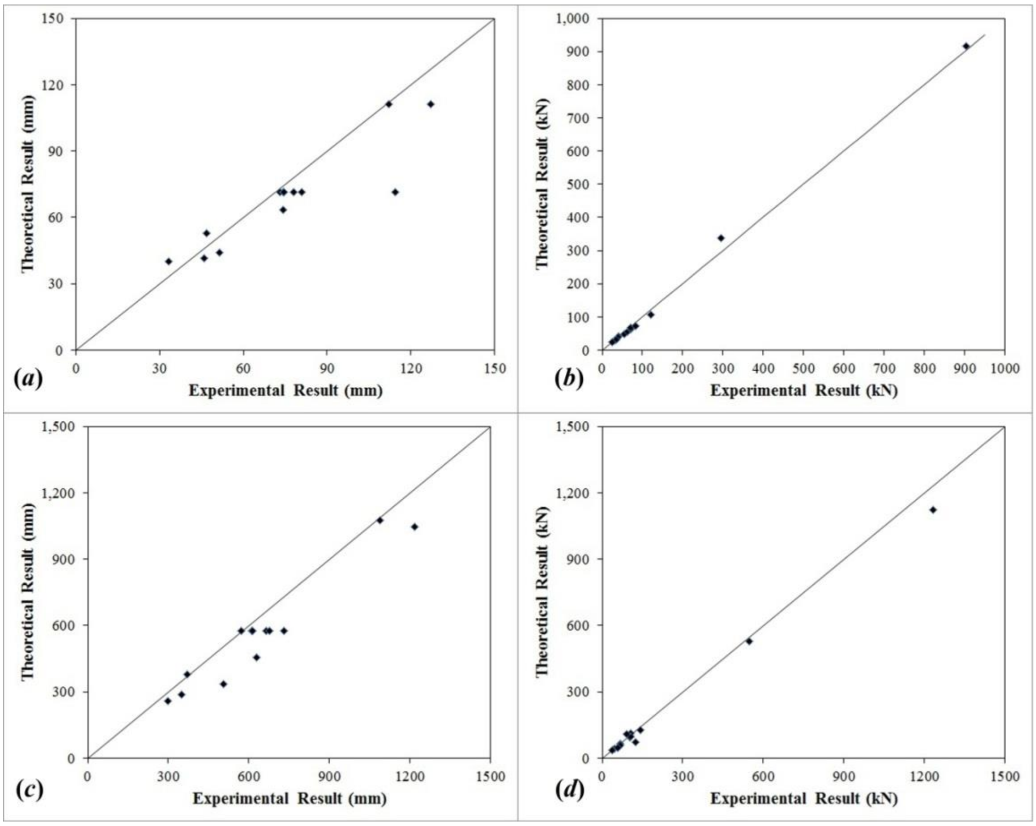

Fig. 6 Comparison of theoretical and experimental results; (a) y_u, (b) P_u, (c) y_{CA}, (d) P_{CA}

the proposed theoretical method can predict the ultimate capacities of the sub-assemblages accurately while correlation coefficients indicate larger discrepancies for displacement estimations but generally the predictions are acceptable.

According to Table 3, the theoretical predictions of compressive arch capacity are mostly accurate. Largest difference is about 14.6% which is obtained for *IMF*. As mentioned before, rotational freedom of the middle columns in real structures are restrained due to the other members in the frame. Hence, the middle joint cannot rotate freely and in beams with similar spans, mostly a symmetric crack pattern occurs (the third assumption). Fig. 7 demonstrates the crack patterns of *IMF* and *SMF* at the end of the compressive arch action (Lew *et al.* 2014). Despite *SMF*, rotation of the middle joint in *IMF* was not restrained completely and as the cracks were concentrated at the weaker (right) side, the joint is rotated toward the other (left) side. Almost symmetric crack pattern in Fig. 7(b) verifies the successful constraints of the middle joint in *SMF*. The mentioned process in *IMF* has happened gradually during the compressive arch stage and hence, prevented from reaching to real compressive arch capacity. Hence, it is expected that the real resistance of *IMF* will be larger in real frame structures. Therefore, in case of having a symmetric failure mode, it is expected to obtain an accurate theoretical prediction.

The theoretical catenary capacity of *S*3 is obtained equal to 71.76 kN while the corresponding experimental resistance is about 124.37 kN. According to the reinforcement detailing of *S*3, a lap splice of bottom bars was used at the middle joint. Hence, two cutoffs in bottom bars were existed

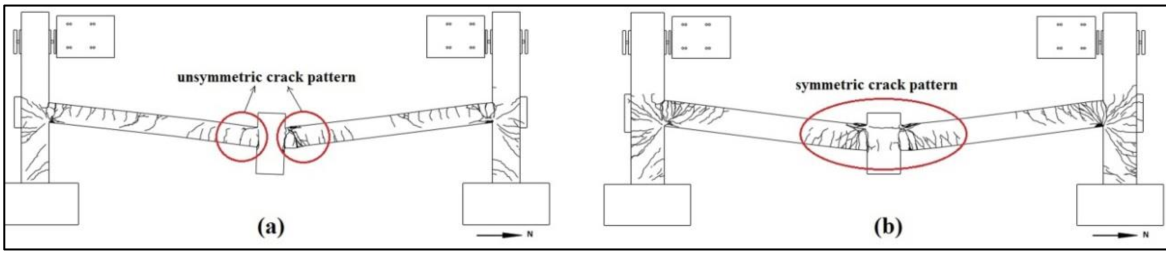

Fig. 7 Crack patterns at the end of compressive arch action Lew *et al.* (2014); (a) *IMF*, and (b) *SMF*

Fig. 8 Local failure modes at the middle joint regions (Yu and Tan 2013): (a) *S*3; and (b) *S*4

at two sides of the joint (Yu and Tan 2013). These cutoffs in tension bars, especially in regions with high shear forces cause stress concentration and consequently, can lead to major inclined cracks at the bar cutoff (Wight and MacGregor 2012). As a result, the location of local failures (plastic hinges) moved from the joint interfaces to the free ends of the splice bars (Yu and Tan 2013). This movement in the location of local failures, which is depicted in Fig. 8, helped the middle joint to have more ductile behavior and hence, larger vertical deflection could be reached (729 mm according to the experiment). This larger deflection leads to larger vertical components of the tensile forces in the longitudinal bars and consequently, larger catenary capacity. These effects are not considered in the theoretical model and hence, the difference between theoretical and experimental capacities is obtained.

According to experiments (Yu and Tan 2013), shear failure of *S8* is occurred due to the short spans and prevented the development of catenary action in the beams. Since shear failure of beams is neglected in the theoretical model, this difference (about 17.7% according to Table 3) between theoretical and experimental capacity of *S8* is obtained. Typical spans in real structures are larger and consequently, shear failure happens rarely in middle beams but it is common for corner beam-column assemblies (Qian and Li 2012, 2013a, b). Hence, the results of *S*8 are less important as a basis for middle beam-column assemblies.

As the mean values in Table 3 indicate, theoretical predictions are mostly less than experiments and hence, it can be concluded that the proposed method is on the safe side in comparison to real values. The smaller theoretical values are obtained due to the hardening of longitudinal steel bars which is neglected in the theoretical method.

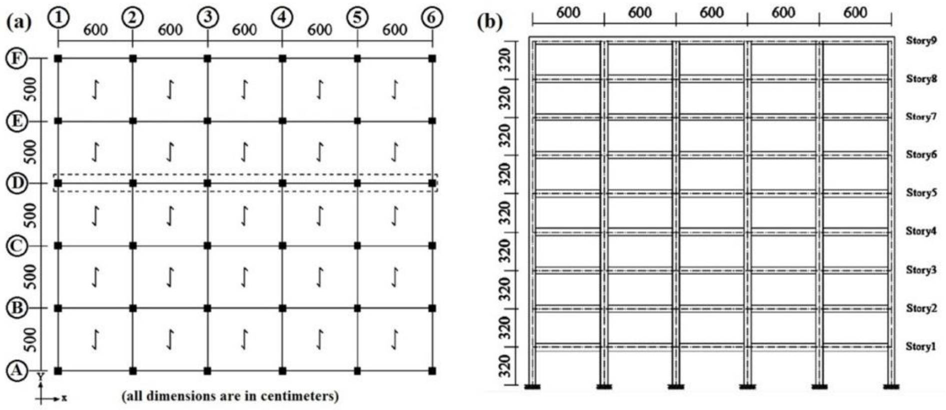

(c)

Story Level		1-3	4-6	7-9
Column	Size	65×65	60×60	55×55
	Reinforcement	24T25	16T25	16T20
Beam	Size	55×45	50×40	45×35
	Top Reinforcement	7 T25	7T25	7T20
	Bottom Reinforcement	5T25	5T25	5T20

Fig. 9 Building Specifications; (a) plan, (b) elevation, and (c) section properties

3.2 Robustness againt progressive collapse

In order to validate the proposed formulation which determines the robustness of a frame against progressive collapse, first a nine story RC frame building is discussed. This building which is designed in accordance with ACI 318-08 (2008) and ASCE 7-05 (2006), is analyzed under a middle column removal scenario. Fig. 9 demonstrates the ground floor plan of the building and specifies the removed column and also lists description of the elements. The uniform dead and live loads equal to 6 kN/m^2 and 2 kN/m^2 are applied to all floors, respectively. Since the present study focuses on RC frames and also the structural system is regular in plan and elevation, only the specified frame in Fig. 9 (frame *D*) is modeled and analyzed and the gravity loads equivalent to the tributary area of the frame are applied. Hence, a two dimensional model is developed using SAP2000 (2013) and a non-linear dynamic procedure is performed under the column removal scenario according to GSA, (2013). The finite element model is constructed based on the details provided by Sasani and Sagiroglu (2008a, b, 2010).

The process of progressive collapse analysis is performed according to Sasani and Sagiroglu (2010) and also in accordance with GSA (2013). Bernoulli beam elements are used to model beams and columns. The end portions of beams and columns within the joints are modeled as rigid zones. Beams have T sections with effective flange width on each side of the web equal to four times the slab thickness. Plastic hinges are assigned to all possible locations where steel bar yielding can occur, including the ends of the elements as well as the reinforcing bar cutoff and bend locations. The characteristics of the plastic hinges are obtained using section analyses of the beams and columns, assuming a plastic hinge length equal to half of the section depth. Geometric nonlinearity (large displacement response) is accounted for. A constant time step equal to 0.001 seconds is used in the dynamic analysis. Rayleigh damping is used to account for damping ratios of 0.05 in the first two modes (primarily vertical vibration). Based on these Sasani and Sagiroglu (2010), firstly the building is analyzed under gravity loads and internal forces (including axial and

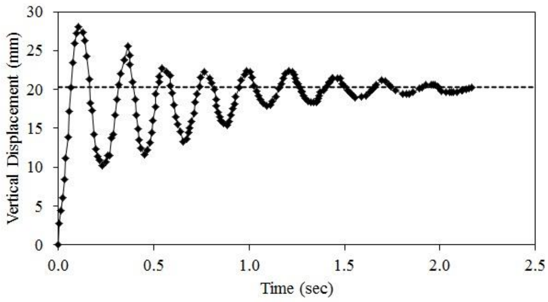

Fig. 10 Displacement time history response of the joint above the removed column

shear forces and flexural and torsional moments) are extracted at top of the column which is being removed. At the second step, the column is removed and the obtained internal loads (at the previous step) are applied at the top of the removed column simulating effects of the column which is eliminated. The building is again analyzed under the gravity loads. The results of these two analyses should be similar. Finally another set of external loads by similar magnitudes but opposite directions in comparison to internal forces of the removed column are applied at top of the column and a nonlinear time history analysis is performed. Applying opposite loads simulates the process of column removal. Hence, responses of the structure could be extracted under column removal analysis. More details on the procedure of the analysis is available in Sasani and Sagiroglu (2010).

Fig. 10 demonstrates the vertical displacement above the removed column where a maximum displacement of 27.9 mm and also a permanent displacement of 20.3 mm are obtained. Axial force of the removed column was 2210 kN before eliminating which transfers to other members. According to experiments (Yu and Tan 2013), when the vertical displacement of the middle joint is around 0.18h to 0.46h, compressive arch capacity of the beams is obtained (h is depth of the beam). In the evaluated building, this ratio is around 0.62h and 0.45h for maximum and permanent displacements, respectively. Hence it could be concluded that under static equilibrium at the end of vibration, the building is probably at the end of the compressive arch stage or at the first of the catenary stage where the catenary forces are not developed yet.

In order to evaluate the robustness of the frame using theoretical formulations, arching and catenary capacities of the beams in different stories are computed using the proposed formulations. Table 4 lists the results for different beams in the frame. Based on the obtained capacities, arching and catenary ratios could be computed according to Eqs. (16)-(17). Regarding the results, λ_1=1.077 and λ_2=0.369 indicate that the compressive arch capacity is obtained and the frame is at the first of the catenary stage which is similar to analytical observations. Although further investigation based on comprehensive analyses is needed in order to reach to a general conclusion, the performed evaluation indicates that the introduced concept could quantify the structural robustness against progressive collapse with an acceptable accuracy.

In a further evaluation, the robustness of the RC frames which investigated sub-assemblages were a part of them, are evaluated using arching and catenary ratios. Since the real value of the column's axial force in these structures was not known, it is calculated based on the reported gravity loads in the references. It is assumed that all the beams in the upper stories have the same sizes and reinforcements. Based on the available descriptions in the references, $S1$ to $S8$ must withstand and transfer the loads corresponding to five stories while IMF and SMF should do the

Table 4 Reinforcement detailing of the building

Story level	Beam sections	Material Properties			P_u (kN)	P_{CA} (kN)	$N^{(a)}$ (kN)	λ_1	λ_2
		f_c (MPa)	f_y (MPa)	f_u (MPa)					
1-3	55×45				337.30	855.50			
4-6	50×40	30	400	600	274.10	837.76	2210	1.077	0.369
7-9	45×35				148.60	525.02			

(a) Axial force in the removed column obtained from simulation analysis

Table 5 Resistance against progressive collapse

Model	Loads (kN/m)				$L_r^{(a)}$ (m)	$n^{(b)}$	$N^{(c)}$ (kN)	Theoretical		Experimental	
	Dead	Live	Dead (roof)	Live (roof)				λ_1	λ_2	λ_1	λ_2
S1								0.99	0.62	1.00	0.60
S2								1.07	0.70	1.08	0.61
S3								0.85	0.58	0.76	0.33
S4								0.75	0.43	0.66	0.40
S5	6.33	7.20	6.33	1.81	3.000	5	186.8	0.67	0.36	0.59	0.40
S6								0.60	0.32	0.59	0.29
S7								0.56	0.41	0.50	0.39
S8								0.39	0.38	0.34	0.45
IMF	34.00	21.90	29.58	5.49	6.096	7	2258.4	1.06	0.68	1.21	0.66
SMF								0.39	0.32	0.40	0.29
P1	4.66	2.26	2.12	0.40	2.100	5	64.5	0.48	0.32	0.45	0.30
P2	6.52	3.16	5.60	0.76	1.500	5	67.7	0.49	0.31	0.42	0.25
M	4.60	2.19	4.00	0.55	1.830	6	70.5	0.54	0.51	0.36	0.35

(a) Removed column's bearing length
(b) Number of floors above the removed column (including roof)
(c) Estimated axial force in the removed column

same duty for seven stories. The continuous model (*M*) of Stinger and Orton (2013) is chosen from a six story building. Since there is not any information about the number of stories in the building which *P*1 and *P*2 are chosen, it is assumed to be a five story structure. These concepts are used to calculate the axial force of the removed column and consequently, the resistance of the structures is computed based on the arching and catenary capacities of the beams. Table 5 presents the results using theoretical and experimental predictions separately. According to these results and based on theoretical predictions, *S*2 and *IMF* cannot resist against progressive collapse using the arching capacity of the beams while the arching capacity in others was enough to withstand against failure. Hence, the catenary capacity of the beams helps the recent models to cease the progression of the failure. The corresponding values based on experimental results also demonstrate the same trend.

In General, the evaluation study indicates that the theoretical predictions, especially the ultimate capacities of RC beams, are in good agreement with experimental data. Therefore, obtaining the behavior of the RC frames only based on a simple theoretical calculation with a good accuracy is the main advantage of the introduced method. Moreover, the introduced procedure presents a quantitative assessment of the structural robustness against progressive collapse which is also evaluated analytically. Consequently, the proposed theoretical method could provide a simple and reliable approach for progressive collapse analysis of RC frames.

4. Conclusions

This paper presents a simplified theoretical method in order to analyze RC frames under the middle column removal scenarios. The proposed method expresses ultimate capacities of the beams and presents a tangible assessment of structural resistance against progression of the failure within the RC frame. A comprehensive parametric study based on the experiments in the literature is carried out in order to validate the proposed method. The main conclusions can be summarized as follows:

- The proposed method provide acceptable prediction for arching and catenary capacities of RC beams;
- Vertical displacements at the middle joint (above the removed column) corresponding to arching and catenary capacities are also computed with an acceptable accuracy;
- The proposed method quantifies robustness of RC frames against progressive and indicates whether or not collapse occurs;
- Theoretical predictions are generally on the safe side in comparison to real values;
- Only un-symmetric failure modes at two sides of the middle joint (above the removed column) can jeopardize the accuracy of the method;
- Being simple, practical, non-iterative and easy to understand are the main characteristics of the presented theoretical method which helps to easily predict the general collapse behavior of RC frames.

However, collapse analysis is a complicated phenomenon and it is needed to pay attention to all the aspects. The proposed method is presented for middle column removal scenarios while corner columns are also very important and critical in RC frames. In short spans, catenary action cannot develop due to probable shear failure. Hence, considering failure modes in catenary capacity of beams is essential. Contribution of slabs is also neglected in the method which will be discussed in the near future by authors.

References

ACI (2008), *Building Code Requirements for Structural Concrete and Commentary,* ACI 318-08, American Concrete Institute, USA.

Almusallam, T.H., Elsanadedy, H.M., Abbas, H., Alsayed, S.H. and Al-Salloum, Y.A. (2010), “Progressive collapse analysis of a RC building subjected to blast loads”, *Struct. Eng. Mech.*, **36**(3), 301-319.

ASCE (2006), *Minimum Design Loads for Buildings and Other Structures*, ASCE/SEI 7-05, Reston, VA.

ASCE (2010), *Minimum Design Loads for Buildings and Other Structures*, ASCE/SEI 7-10, Reston, VA.

Bao, Y. and Kunnath, S.K. (2010), “Simplified progressive collapse simulation of RC frame-wall structures”, *Eng. Struct*., **32**(10), 3153-3162.

Bao, Y., Kunnath, S.K., El-Tawil, S. and Lew, H.S. (2008), “Macromodel-based simulation of progressive collapse: RC frame structures”, *J. Struct. Eng.,* ASCE, **134**(7), 1079-1091.

Bao, Y., Lew, H.S. and Kunnath, S.K. (2014), “Modeling of reinforced concrete assemblies under column-

removal scenario", *J. Struct. Eng.*, ASCE, **140**(1), 04013026.
Christiansen, K.P. (1963), "The effect of membrane stresses on the ultimate strength of an interior panel in a reinforced concrete slab", *Struct. Eng.*, **41**(8), 261-265.
GSA (2013), *Alternate Path Analysis and Design Guidelines for Progressive Collapse Resistance*, General Services Administration, Washington DC., USA.
Hognestad, E., Hanson, N.W. and Mchenry D. (1955), "Concrete stress distribution in ultimate strength design", *J. Am. Conc. Inst. Proc*., **52**(6), 455-479.
Hon, A., Taplin, G. and Al-Mahaidi, R.S. (2005), "Strength of reinforced concrete bridge decks under compressive membrane action", *ACI Struct. J.*, **102**(3), 1-11.
Jian, H. and Zheng, Y. (2014), "Simplified models of progressive collapse response and progressive collapse-resisting capacity curve of RC beam-column substructures", *J. Perform. Constr. Facil.*, ASCE, **28**(4), 04014008.
Karimiyan, S., Kashan, A.H. and Karimiyan, M., (2014), "Progressive collapse vulnerability in 6-Story RC symmetric and asymmetric buildings under earthquake loads", *Earthq. Struct.*, **6**(5), 473-494.
Kim, J., Lee, S. and Min, K.W. (2014), "Design of MR dampers to prevent progressive collapse of moment frames", *Struct. Eng. Mech.*, **52**(2), 291-306.
Lew, H.S., Bao, Y., Pujol, S. and Sozen, M.A. (2014), "Experimental study of reinforced concrete assemblies under column removal scenario", *ACI Struct. J.*, **111**(4), 881-892.
Li, J. and Hao, H. (2013), "Numerical study of structural progressive collapse using substructure technique", *Eng. Struct*., **52**, 101-113.
Long, X., Yuan, W., Tan, K.H. and Lee, C.K. (2013), "A superelement formulation for efficient structural analysis in progressive collapse", *Struct. Eng. Mech.*, **48**(3), 309-331.
Mattock, A.H., Kriz L.B. and Hognestad, E., (1961), "Rectangular concrete stress distribution in ultimate strength design", *J. Am. Conc. Inst*., **57**(8), 875-926.
McDowell, E.L., McKee, K.E. and Sevin, E. (1956), "Arching action theory of masonry walls", *J. Struct. Div.*, ASCE, **82**(ST2), 915.
Menchel, K., Massart, T.J. and Bouillard, Ph. (2011), "Identification of progressive collapse pushover based on a kinetic energy criterion", *Struct. Eng. Mech.*, **39**(3), 427-447.
Qian, K. and Li, B. (2012), "Dynamic performance of RC beam-column substructures under the scenario of the loss of a corner column-Experimental results", *Eng. Struct*., **42**, 154-167.
Qian, K. and Li, B. (2013a), "Analytical evaluation of the vulnerability of RC frames for progressive collapse caused by the loss of a corner column", *J. Perform. Constr. Facil.*, ASCE, **29**(1), 04014025.
Qian, K. and Li, B. (2013b), "Performance of three-dimensional reinforced concrete beam-column substructures under loss of a corner column scenario", *J. Struct. Eng.*, ASCE, **139**(4), 584-594.
Qian, K., Li, B. and Ma, J. X. (2014) "Load-carrying mechanism to resist progressive collapse of RC buildings", *J. Struct. Eng.*, ASCE, **141**(2), 04014107.
Rankin, G.I.B. and Long, A.E. (1997), "Arching action strength enhancement in laterally-restrained slab strips", *Struct. Bldg. (ICE)*, **122**, November, 461-467.
SAP2000 (2013), *Three Dimensional Static and Dynamic Finite Element Analysis and Design of Structures*, Analysis Reference, Version 16.0.0, Computer and Structures, Inc., Berkeley, CA.
Sasani, M. (2008), "Response of a reinforced concrete infilled-frame structure to removal of two adjacent columns", *Eng. Struct*., **30**(9), 2478-2491.
Sasani, M. and Sagiroglu, S. (2008a), "Progressive collapse of RC structures: a multi-hazard perspective", *ACI Struct. J.*, **105**(1), 96-103.
Sasani, M. and Sagiroglu, S. (2008b), "Progressive collapse resistance of Hotel San Diego", *J. Struct. Eng.*, ASCE, **134**(3), 474-88.
Sasani, M. and Sagiroglu, S. (2010), "Gravity load redistribution and progressive collapse resistance of a 20-story RC structure following loss of an interior column", *ACI Struct. J.*, **107**(6), 636-644.
Sasani, M., Bazan, M. and Sagiroglu, S. (2007), "Experimental and analytical progressive collapse evaluation of an actual reinforced concrete structure", *ACI Struct. J.*, **104**(6), 731-739.
Sasani, M., Kazemi, A., Sagiroglu, S. and Forest, S. (2011a), "Progressive collapse resistance of an actual

11-story structure subjected to severe initial damage", *J. Struct. Eng.*, ASCE, **137**(9), 893-902.

Sasani, M., Werner, A., and Kazemi, A. (2011b), "Bar fracture modeling in progressive collapse analysis of reinforced concrete structures", *Eng. Struct.*, **33**(2), 401-409.

Stinger, S.M. and Orton, S.L. (2013) "Experimental evaluation of disproportionate collapse resistance in reinforced concrete frames", *ACI Struct. J.*, **110**(3), 521-530.

Su, Y., Tian, Y. and Song, X. (2009), "Progressive collapse resistance of axially-restrained frame beams", *ACI Struct. J.*, **106**(5), 600-607.

Tavakoli, H. and Akbarpoor, S., (2014), "Effect of brick infill panel on the seismic safety of reinforced concrete frames under progressive collapse", *Comput. Concrete*, **13**(6), 749-764.

Weerheijm, J., Mediavilla, J. and VanDoormaal, J.C.A.M. (2009), "Explosive loading of multi storey RC buildings: Dynamic response and progressive collape", *Struct. Eng. Mech.*, **32**(2), 193-212.

Wight, J.K. and MacGregor, J.G. (2012), *Reinforced Concrete: Mechanics and Design*, 6th Edition, Pearson Prentice Hall.

Yagob, O., Galal, K. and Naumoski, N. (2009), "Progressive collapse of reinforced concrete structures", *Struct. Eng. Mech.*, **32**(6), 771-786.

Yi, W.J., He, Q.F., Xiao, Y. and Kunnath, S.K. (2008), "Experimental study on progressive collapse-resistant behavior of reinforced concrete frame structures", *ACI Struct. J.*, **105**(4), 433-439.

Yu, J. and Tan, K.H. (2011), "Experimental and numerical investigation on progressive collapse resistance of reinforced concrete beam column sub-assemblages", *Eng. Struct.*, **55**, 90-106.

Yu, J. and Tan, K.H. (2013), "Structural behavior of RC beam-column sub-assemblages under a middle column removal scenario", *J. Struct. Eng.*, ASCE, **139**(2), 233-250.

Yu, J. and Tan, K.H. (2014), "Analytical model for the capacity of compressive arch action of reinforced concrete sub-assemblages", *Mag. Concrete Res. (ICE)*, **66**(3), 109-126.

Yu, J., Rinder, T., Stolz, A., Tan, K. and Riedel, W. (2014), "Dynamic progressive collapse of an RC assemblage induced by contact detonation", *J. Struct. Eng.*, ASCE, **140**(6), 04014014.

CC